# R3-A.1: Millimeter Wave Whole Body Scanning Radar Hardware for Advanced Imaging Technology (AIT)

## I. PARTICIPANTS

| Faculty/Staff | | | |
|---|---|---|---|
| **Name** | **Title** | **Institution** | **Email** |
| Carey Rappaport | Co-PI | NEU | rappaport@neu.edu |
| Jose Martinez | Co-PI | NEU | jmartine@ece.neu.edu |
| Borja Gonzalez-Valdes | Post-Doc | NEU | bgonzale@ece.neu.edu |
| Yuri Alvarez | Visiting Faculty | NEU | yurilope@gmail.com |
| Richard Moore | Consultant | MGH | Moore.Richard@mgh.harvard.edu |
| Dan Busuioc | Consultant | NEU | db.ipaq@gmail.com |
| **Graduate, Undergraduate and REU Students** | | | |
| **Name** | **Degree Pursued** | **Institution** | **Month/Year of Graduation** |
| Matthew Nickerson | BS | NEU | 5/2016 |
| Nigil Lee | BS | NEU | 5/2017 |
| Scott Pitas | BS | NEU | 5/2015 |
| Thurston Brevett | BS | NEU | 5/2018 |
| Michael Woulfe | BS | NEU | 5/2018 |
| Matthew Tivnan | BS | NEU | 5/2017 |
| Andrew Mello | BS | NEU | 5/2017 |
| Sara Davila | BS | NEU | 5/2017 |
| Zamir Johl | BS | NEU | 5/2018 |
| Abeco Jean Claude Rwakabuba | REU | Middlesex CC | 5/2016 |
| Kurt Jaisle | REU | NEU | 5/2019 |
| Jacob Messner | REU | NEU | 5/2019 |
| Lingrui Zhong. | NSF Young Scholar | Lexington HS | 6/2016 |
| Shiva Nathan | NSF Young Scholar | Westford Academy HS | 6/2016 |

## II. PROJECT DESCRIPTION

### *A. Overview and Significance*

As people enter secure areas, it is important that they be scanned to ensure that they are not entering with weapons or explosives. In addition to airport departure gates; office buildings, stadiums and arenas must have fast, accurate, non-intrusive means of detecting threats concealed under clothing.

The R3-A.1 Whole Body Imaging project developed an improved multi-modality, portal-based passenger

screening system. The system developed with millimeter-wave (mm-wave) nearfield imaging radar in the 56-64 GHz frequency band makes use of the patented Blade Beam reflector transmitting antenna, along with a multistatic array of receiving antenna for artifact-free imaging. The Blade Beam produces a narrow target illumination to allow accurate stacked 2D reconstructions of the 3D surface.

Mm-waves pass though clothing readily, but can identify dangerous objects attached to the body. Current state-of-the-art millimeter wave portal imaging systems are mostly based on monostatic radar. Although these systems are inherently fast, they present some disadvantages, including reconstruction artifacts, such as dihedral effects and misrepresenting sudden indentations and protrusions due to the monostatic nature of the collected electric field data, and a lack of quantitative range of depth information display.

### *B. State-of-the-Art and Technical Approach*

The industry-standard AIT scanner uses multi-monostatic low mm-wave frequency radar and decades-old algorithms to provide images of body surfaces with affixed objects [1, 2]. It cannot characterize dielectric materials, provide surface depth information, and suffers from dihedral artifacts and non-specular drop-outs. Research in R3-A.1 addresses these deficiencies by employing multiple receivers for a single high-gain illuminating transmitter [3-6]. Results of this project show that artifacts are eliminated, depth information is readily available and extremely useful, and weak dielectric objects are characterized by well-reconstructed depressions in the body surface. Due to the fact that specular drop-outs have not been solved with the employed reflector geometry, this project will end in December 2015 and be merged with project R3-A.3, which uses multiple transmitters.

We designed a custom reflector-based antenna for focusing the field on a narrow vertical slit to provide for two dimensional illumination [7-10]. This reduces both the hardware and algorithmic load for AIT sensing. By stacking individually reconstructed slices, we avoid the simultaneous computation of field contributions from multiple height, which speeds up data acquisition and imaging by several orders of magnitude. We employed a moving receiver, which acted like a synthetic aperture radar, with multistatic array sensing to avoid dihedral artifacts from body crevices and reduce false alarms. The multistatic configuration also extends imaging performance by giving multiple views of each body surface pixel. Our radar hardware uses inexpensive, Commercial Off-The-Shelf (COTS) communication modules repurposed for nearfield imaging. This further reduces the cost of mm-wave AIT and make it possible to build an advanced system for general purpose security use.

### *C. Major Contributions*

Using the hardware developed during Year 1, we have conducted an extensive experimental campaign to determine the capabilities and limitations of the Blade Beam. Although the single transmitter configuration limits the tilt or curvature of the target object, there was still some reasonable success at imaging relevant 3D objects by stacking 2D images. Also, we experimentally validated the dielectric object characterization algorithm developed in R3-A.2.

An example of this capability involves the target shown in Figure 1 on the next page. This target is a flat metal box surface with two square cross-section anomalies attached, one metallic, and one a wax explosive simulant. This simulates a metallic object and an explosive taped to a flat portion of skin.

The Blade Beam illuminates narrow horizontal slices of the target. Each slice is reconstructed, and then stacked with adjacent slices to form a surface representation. Figure 2a on the next page shows the image of the slice taken near the bottom of the target in Figure 1, illuminating a slice that includes the square metal anomaly. With the radar at the bottom, the metal anomaly is observed as the bump extending downward, closer to the radar (with less range). Figure 2b on the next page is the reconstruction of a slice near the top, illuminating the dielectric anomaly. In this case, the response at the position of the dielectric appears as

being further from the radar, (with greater range). As expected, the response is primarily from the metal surface behind the dielectric, but due to the slower wave propagation velocity in the dielectric, this response is delayed, and the image is farther from the radar. The ground truth is shown in green, with the backing surface depression corresponding to the reduced velocity in the dielectric as indicated with the blue rectangle.

**Figure 1: Target object consisting of a flat metal surface with a square metallic and a square dielectric anomaly.**

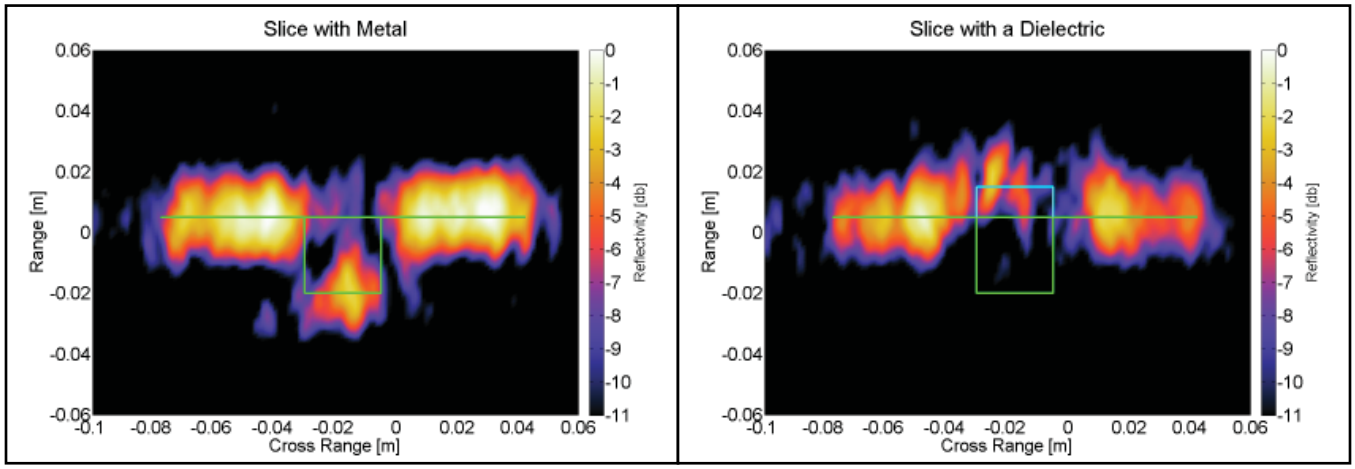


a) b)

**Figure 2: 2D image of narrowly illuminated slice of target in Figure 1 for: a) square metallic anomaly, and b) square dielectric anomaly, with ground truth shown in green.**

Figure 3 on the next page shows the same image, with the surface profile reconstructed (green curves). The profile is determined by selecting the range with the highest intensity image response for each cross range position. Note the excellent agreement for the metallic anomaly and the reasonable surface depression for the dielectric target.

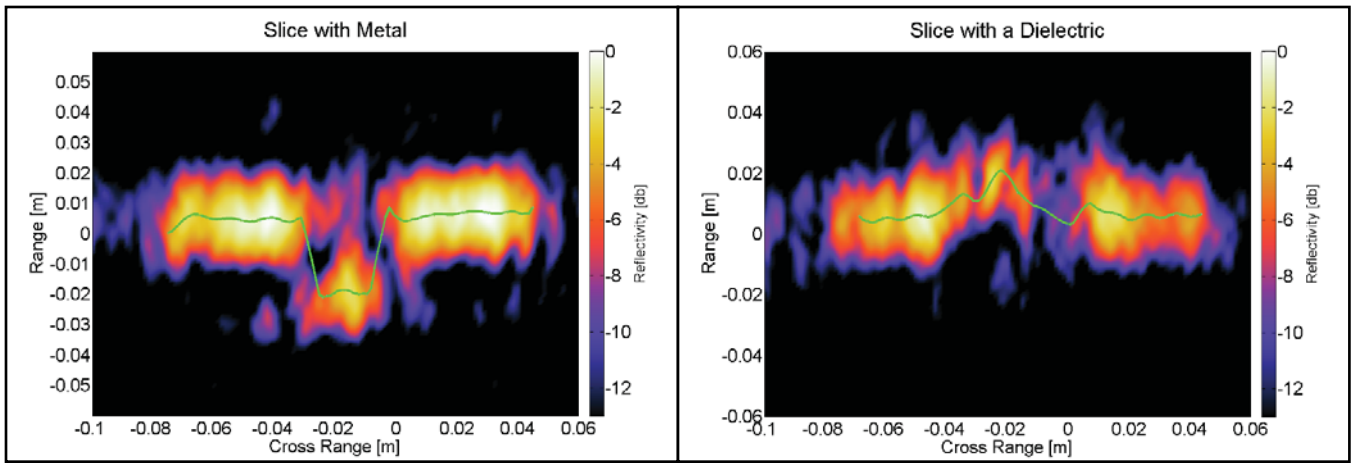


a) b)

**Figure 3: 2D slice images of Figure 2 with surface profile, shown in green, reconstructed for: a) square metallic anomaly, and b) square dielectric anomaly.**

Stacking mulitple 2D slices produces a full surface image, as shown in Figure 4. Note the sizes, shapes, and positions of the anomalies are in good agreement with the true configuration of Figure 1, with the added feature that the dielectric appears to be recessed (white color coded, corresponding to greater range).

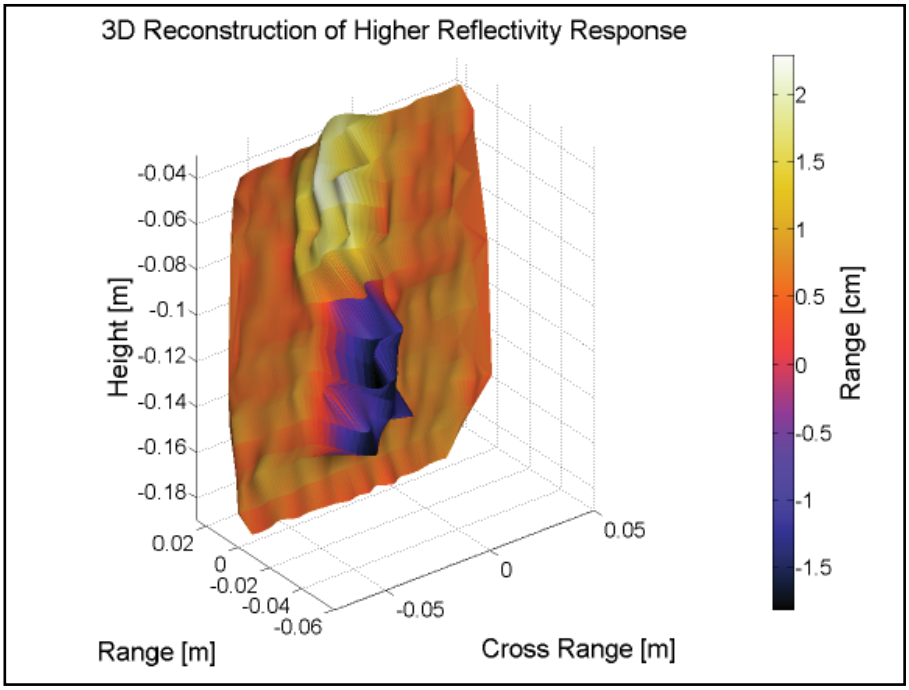


**Figure 4: 3D full surface reconstruction of target object of Figure 1, using multiple slice images similar to Figure 3.**

A more challenging and realistic target was also tested. In this case, the background was a curved metal surface with the approximate size and curvature of a human torso. Once again a metallic object and a dielectric explosive simulant were affixed to the background, but this time the entire object was covered by a thick cotton sweatshirt. Figure 5 on the next page shows the covered and uncovered target.


**Figure 5: Torso simulant with metal and dielectric explosive simulants.**

Note the curvature of the curved metal surface, which follows the true shape approximating a human chest. This curvature is accurately reconstructed in the image of the upper slice, labeled "Control Slice" in Figure 6a on the next page. The reconstructed surface is indicated with the green curve. The second image, Figure 6b on the next page, "Metal Slice," corresponds to illumination of the middle psortion of the torso target that has a 3 cm thick metal anomaly, centered 6 cm to the right of the centerline. This anomaly appears as a downward protrusion (closer to the radar at the bottom) which is highlighted with a white dashed circle. The third image, Figure 6c on the next page shows the depression at -12cm, characteristic of a dielectric object. The depression is about $D_{depres}$ = 2 cm deep, which corresponds to the expected value for a 3 cm ($D_{thick}$) thick slab of material with dielectric constant $\varepsilon_{diel}$ = 2.9, given by the equation:

$$D_{depres} = D_{thick} \left( \sqrt{\varepsilon_{diel}} - 1 \right)$$

In order to determine both the dielectric slab thickness and its dielectric constant simultaneously with a single measurement, it is important to use a high-resolution algorithm. As there are two unknowns to be determined, there must be two observed aspects in the reconstructed image. These are the depression of the backing surface response and the front dielectric object surface response. Unfortunately, for weak dielectrics, this initial front surface response is weak, so weak that it does not appear on the image with typical -12 dB reflectivity scale on Figure 2b. If the reflectivity scale is increased to -35 dB, as indicated in Figure 7a on the following page, the front surface response corresponding to the dielectric becomes readily apparent. However, it is unclear whether this medium level -15dB response is due to a dielectric object or just a noisy extended response from the backing surface.

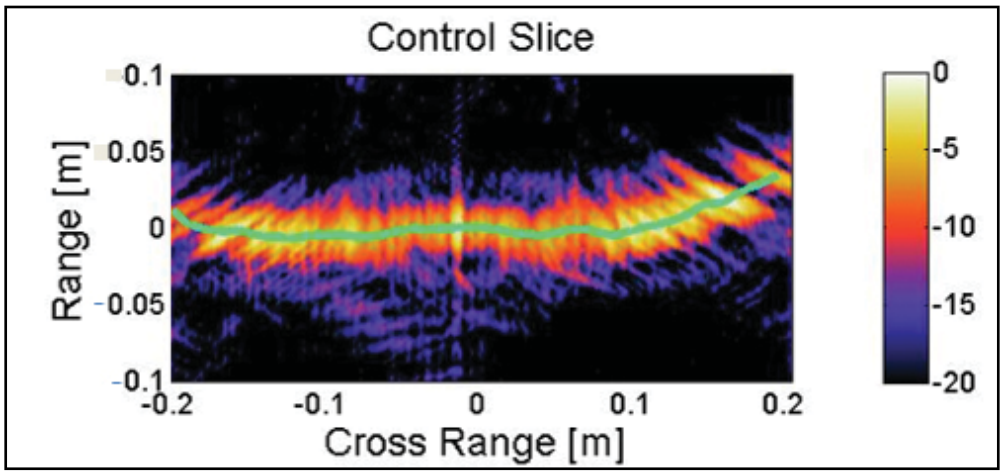


a)

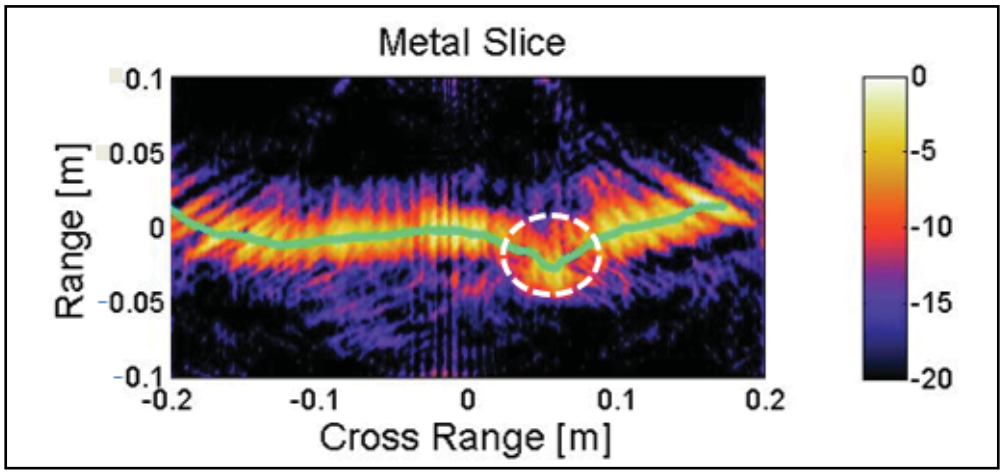


b)

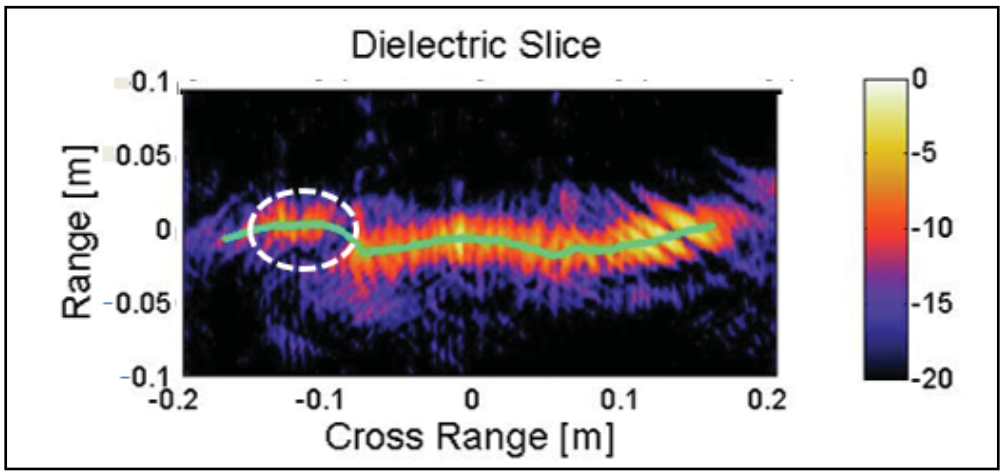


c)

**Figure 6: Reconstructions of three slice illuminations of torso simulant for a) no anomaly, b) square cross section metal box anomaly, and c) square dielectric anomaly. Derived contour indicated by green curve.**

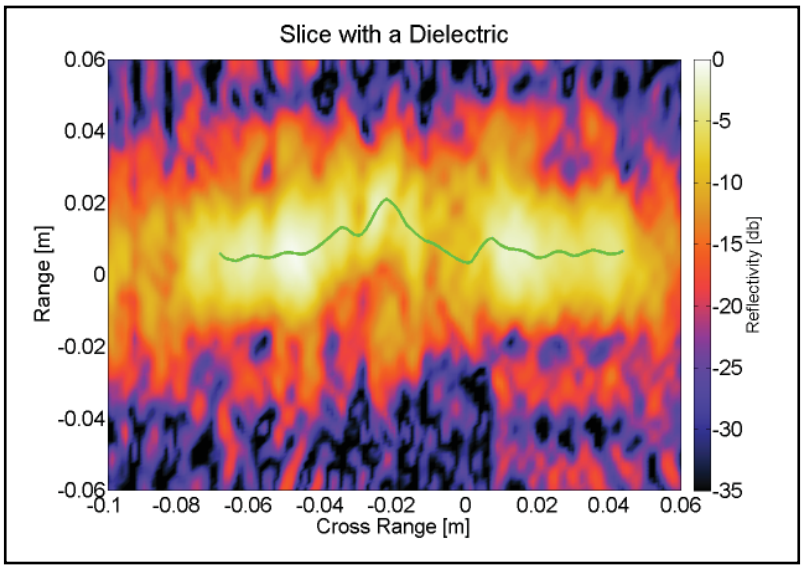


a)

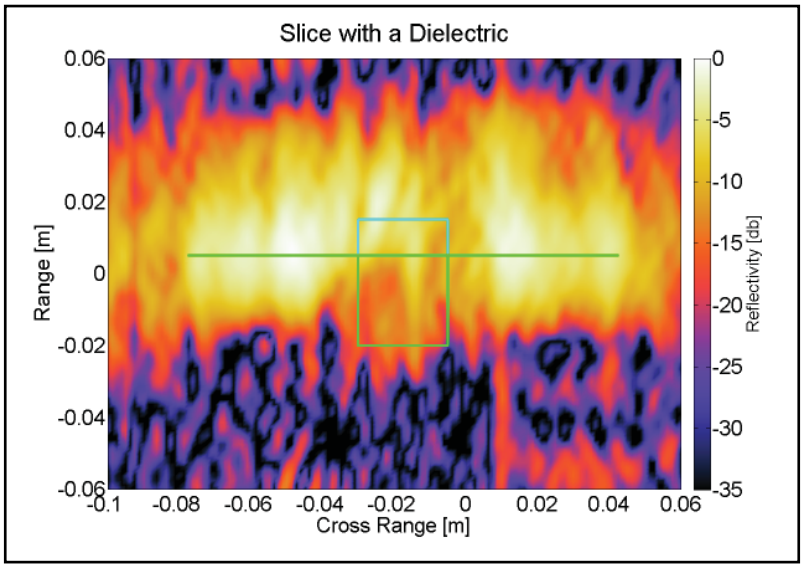


b)

**Figure 7: Reconstructions of a square dielectric bar on a planar metal backing a) full 7 GHz bandwidth, showing derived contour indicated by green curve b) with bandwidth reduced to 4 GHz and ground truth shown in green and backing depression in cyan.**

To distinguish a dielectric object response, a new method has been developed. Using the same measurement data that generates the image in Figure 7a, but restricting the frequency band to just 4 GHz instead of the usual 7 GHz, the sidelobe structure of the backing surface is altered. The entire pattern spreads out in range, widening the peaks,widening position of the nulls and the sidelobes relative to the peaks. As shown in Figure 7b, the -17 dB sidelobes to the right and left of the dielectric anomaly have shifted from -0.03 to -0.055 cm in range. The peak position is independent of bandwidth, so the dielectric front surface response is still at -0.02 cm (though smeared out). Since the response at range -0.02 is unchanged for the reduced bandwidth image, it must correspond to a real interface, rather than a sidelobe. As such, it is declared to be the front surface of the dielectric object. The ground truth is indicated in Figure 7b by the square green box, and the depresson of the backing reflection is shown with the cyan rectangle. Knowing the true thickness of the dielectric ob-

ject $D_{thick}$ (from the distance between the front and nominal backing surfaces), and the depression $D_{depres}$, the above equation can be simply inverted to give a correct estimate of the dielectric constant. Note that we use a subset of previously collected data over a reduced bandwith for this algorithm; no additional meaurements are necessary.

*D. Research Milestones Accomplished (in lifetime of project)*

- Adapted COTS mm-wave communications chip as radar module.
- Demonstrated multistatic radar sensing improvement with synthetic array of receivers.
- Proved dihedral artifact reduction with multistatic radar.
- Showed how reflector antenna can increase aperture, focus vertically into a blade beam, and increase signal power.
- Adapted hardware to reduce computational reconstruction burden.
- Demonstrated weak dielectric characterization through experimentation.

*E. Future Plans*

This project will end in December 2015. It will be merged with project R3-A.3.

## III. EDUCATION AND WORKFORCE DEVELOPMENT ACTIVITY

*A. Student Internships, Jobs or Research Opportunities*

Research Experience for Undergraduates (REU) students: 2014: Abeco Jean Claude Rwakabuba (minority student) from Middlesex Community College; Thurston Brevett (minority student) Northeastern University; 2015: Kurt Jaisle, Jacob Messner, Northeastern University

Undergraduate students currently participating in this project: Michael Woulfe, Andrew Mello, Zamir Johl, and Sara Davila.

*B. Interactions and Outreach to K-12, Community College, Minority Serving Instituion Students or Faculty*

NSF Young Scholars (high school students): Shiva Nathan and Lingrui Zhong.

*C. Workforce Development*

Two completed Career Development Grant Master's degree students in the 2014 – 2015 academic year.

- Alex Showalter-Bucher, (2014), now employed at MIT Lincoln Labs.
- Michael Collins, (2014), now employed at the Center for Marine Research and Experimentation in La Spezia, Italy.

## IV. RELEVANCE AND TRANSITION

*A. Relevance of Research to the DHS Enterprise*

- Custom developed AIT hardware speeds scanning: stacked 2D imaging reduces hardware requirement by a factor of 100 (for 1 cm resolution), and computation by a factor of 10,000, without affecting ROC curve.
- Commercial Off-The-Shelf (COTS) communication modules repurposed as AIT screening radar saves

money and allows for general security use: radar module cost savings from $12,000 to $150, while maintaining performance (PD, PFA) and speed (passenger throughput).

- Multistatic configuration extends imaging performance by giving multiple views of each body surface pixel, improving the signal to noise (potentially PF, PFA) and reducing image artifacts (dihedral artifacts eliminated).
- The net effect of these improvements will provide better detection, reduce image artifacts, reduced cost while maintaining PD, PFA and passenger throughput.

*B. Potential for Transition*

- Inexpensive COTS communication modules are currently being used in the Rapiscan, Inc. JAII project as a feasibility study for on-the-move hallway AIT sensor development, so that the communications modules can be easily transitioned to the commercialization partner.
- Dielectric characterization exhibiting reconstructed depression in the body surface will be tested as part of the L3, Inc. ProVision system funded by a pending DHS task order. The data for the research comes from the commercialization partner, so the science and implementation will directly apply, but the commercialization partner will have to implement the commercialization of the software.
- Rethinking of multistatic sensor configuration using ray analysis with increased viability of Rohde and Schwarz, Inc. walk-through tunnel concept. It has been determined that signals must be received from transmitters on the other side of the subject to image 360 deg. It is now necessary to find the best double-sided multistatic configuration.

*C. Transition Pathway*

Joint proposals (JAII, DHS BOA) and demonstration of research concepts with industry systems, testing, and validation on company hardware will immerse users and potential commercialization partners in the transition process and expedite commercialization. This project will terminate in December 2015. The results and lessons learned will be incorporated into project R3-A.3.

*D. Customer Connections*

- Simon Pongratz: L-3 Communications Corp., Woburn, MA
- Shiva Kumar, Ed Morton, Dan Strellis: Rapiscan Laboratories Inc., Burlington, MA

## V. PROJECT DOCUMENTATION

*A. Peer Reviewed Journal Articles*

1. Y. Alvarez, B. Valdes, J. A. Martinez-Lorenzo, F. Las-Heras and C. M. Rappaport. “SAR imaging-based techniques for Low Permittivity Lossless Dielectric Bodies Characterization,” Antennas and Propagation Magazine, Vol. 57 no. 2, April 2015, pp. 267 - 276.

*B. Peer Reviewed Conference Proceedings*

1. Gonzalez-Valdes, B., Martinez-Lorenzo, J. A., and Rappaport, C., “On-the-Move Active Millimeter Wave Interrogation System Using a Hallway of Multiple Transmitters and Receivers,” IEEE International Antennas and Propagation Symposium, July 2014, pp. 1107-1108.
2. Rappaport, C., González-Valdés, B., and Martínez-Lorenzo, J. A., “Advanced Portal-Based Multistatic

Millimeter-Wave Radar Imaging for Person Security Screening," IEEE International Carnahan Conference on Security Technology, Rome, Italy, October 14, 2014, 3 pages.

*C. Other Presentations*

1. Seminars
   a. Carey Rappaport, "Hardware and Algorithms for Low-Cost, Multistatic Millimeter Wave Radar Whole Body Scanning", July 31, 2014, Telmarc presentation.
   b. Carey Rappaport, "Radar Airport Passenger Security Scanners, Radar Tunnel Detection, Radar Insect Infestation Detection", September 17, 2014, Gordon Scholars' Talk.

*D. Student Theses or Dissertations*

1. Michael Collins, Northeastern University Electrical and Computer Engineering Master's thesis: DETECTING BODY CAVITY BOMBS WITH NUCLEAR QUADRUPOLE RESONANCE, August, 2014.

*E. Technology Transfer/Patents*

1. Patent Applications Filed
   a. Doubly Shaped Reflector Transmitting Antenna for Millimeter-Wave Security Scanning System, filed 3/2015, patent pending.
   b. Modular Superheterodyne Stepped Frequency Radar System for Imaging, 7/15/2014, INV-14002.02, patent pending.

## VI. REFERENCES

[1] D. Sheen, D. McMakin, and T. Hall, "Three-Dimensional Millimeter-Wave Imaging for Concealed Weapon Detection," IEEE T. Microwave Theory and Techniques, vol. 49, no. 9, pp. 1581-1592, Sept. 2001.
[2] D. M. Sheen, D. L., McMakin, T. E. Hall, "Combined illumination cylindrical millimeter-wave imaging technique for concealed weapon detection," AeroSense, International Society for Optics and Photonics, pp. 52-60, July 2000.
[3] S. S. Ahmed, A. Schiessl, F. Gumbmann, M. Tiebout, S. Methfessel, L. Schmidt, "Advanced microwave imaging," IEEE Microwave Magazine, Vol. 13, No. 6, pp. 26-43, 2012.
[4] S. S. Ahmed, "Personnel screening with advanced multistatic imaging technology," SPIE Defense, Security, and Sensing. International Society for Optics and Photonics, 2013.
[5] M. Soumekh, "Bistatic Synthetic Aperture Radar Inversion with Application in Dynamic Object Imaging", IEEE Transactions on Signal Processing, Vol. 39, No. 9, September 1991, pp 2044-2055.
[6] Cooper, K.B.; Dengler, R.J.; Llombart, N.; Thomas, B.; Chattopadhyay, G.; Siegel, P.H., "THz Imaging Radar for Standoff Personnel Screening," IEEE T. Terahertz Science and Technology, , vol.1, no.1, pp.169-182, Sept. 2011.
[7] Rappaport, C.M.; Gonzalez-Valdes, B., "The blade beam reflector antenna for stacked nearfield millimeter-wave imaging," IEEE Antennas and Propagation Society Int'l Symp. , vol., no., pp.1-2, 8-14 July 2012
[8] Alvarez, Y.; Gonzalez-Valdes, B.; Ángel Martinez, J.; Las-Heras, F.; Rappaport, C.M., "3D Whole Body Imaging for Detecting Explosive-Related Threats," IEEE T. Antennas and Propagation, vol.60, no.9, pp. 4453,4458, Sept. 2012.

[9] B. Gonzalez-Valdes, Y. Alvarez, J. A. Martinez, F. Las-Heras, C. M. Rappaport, “On the Use of Improved Imaging Techniques for the Development of a Multistatic Three-Dimensional Millimeter-Wave Portal for Personnel Screening,” Progress In Electromagnetics Research, PIER, Vol. 138, pp. 83-98, 2013.

[10] Martinez-Lorenzo, J.A; Gonzalez-Valdes, B.; Rappaport, C.; Gutierrez Meana, J.; Garcia Pino, A, “Reconstructing Distortions on Reflector.

*This page intentionally left blank.*